

Article

Stochastic Evaluation of Cutting Tool Load and Surface Quality during Milling of HPL

Karel Frydryšek^{1,2,*}, Ondřej Skoupý^{1,2}, Ivan Mrkvica³, Aneta Slaninková³, Jiří Kratochvíl³, Tibor Jurga³, Miroslav Vlk⁴, Pavel Krpec⁵, Roman Madeja^{2,6}, Miroslav Havlíček⁷, Dana Stančková⁸, Jana Pometlová^{2,6} and Josef Hlinka^{9,10}

- ¹ Department of Applied Mechanics, Faculty of Mechanical Engineering, VSB—Technical University of Ostrava, 17. Listopadu 2172/15, 708 00 Ostrava, Czech Republic
 - ² Institute of Emergency Medicine, Faculty of Medicine, University of Ostrava, Syllabova 19, 703 00 Ostrava, Czech Republic
 - ³ Department of Machining, Assembly and Engineering Metrology, Faculty of Mechanical Engineering, VSB—Technical University of Ostrava, 17. Listopadu 2172/15, 708 00 Ostrava, Czech Republic
 - ⁴ VYDONA s.r.o., Novosady 1501, 769 01 Holešov, Czech Republic
 - ⁵ V-NASS, a.s., Halasova 2938/1a, 703 00 Ostrava, Czech Republic
 - ⁶ Trauma Center, University Hospital Ostrava, 17. Listopadu 1790, 708 52 Ostrava, Czech Republic
 - ⁷ Medin, a.s, Vlachovicka 619, 592 31 Nové Město na Moravě, Czech Republic
 - ⁸ Department of Machining and Manufacturing Technologies, Faculty of Mechanical Engineering, University of Žilina, Univerzitná 8215/1, 010 26 Žilina, Slovakia
 - ⁹ Department of Materials Engineering, Faculty of Materials and Technology, VSB—Technical University of Ostrava, 17. Listopadu 2172/15, 708 00 Ostrava, Czech Republic
 - ¹⁰ Centre for Advanced Innovation Technologies, VSB—Technical University of Ostrava, 17. Listopadu 2172/15, 708 00 Ostrava, Czech Republic
- * Correspondence: karel.frydrysek@vsb.cz



Citation: Frydryšek, K.; Skoupý, O.; Mrkvica, I.; Slaninková, A.; Kratochvíl, J.; Jurga, T.; Vlk, M.; Krpec, P.; Madeja, R.; Havlíček, M.; et al. Stochastic Evaluation of Cutting Tool Load and Surface Quality during Milling of HPL. *Appl. Sci.* **2022**, *12*, 12523. <https://doi.org/10.3390/app122412523>

Academic Editor: Mark J. Jackson

Received: 10 October 2022

Accepted: 28 November 2022

Published: 7 December 2022

Publisher's Note: MDPI stays neutral with regard to jurisdictional claims in published maps and institutional affiliations.



Copyright: © 2022 by the authors. Licensee MDPI, Basel, Switzerland. This article is an open access article distributed under the terms and conditions of the Creative Commons Attribution (CC BY) license (<https://creativecommons.org/licenses/by/4.0/>).

Abstract: The topic of the article concerns the mechanics of machining plastics and their machined surface. This article deals with measurements and their stochastic (probabilistic) evaluation of the force and moment loading of the machine tools and workpiece. It also deals with the quality of the machined surface in relation to its surface roughness and surface integrity. Measurements were made under different cutting conditions on a CNC milling machine using a newly designed cutter with straight teeth. The statistical evaluation is presented by bounded histograms and basic statistical characteristics that give a realistic idea of the machining process. The practical focus of the experiments is on the milling of HPL (high-pressure plastic–laminate composite material). The listed procedures can also be applied to other materials and machining methods, and can be used for numerical modelling, setting the optimum parameters of machining technology, or for the design of cutting tools. Numerical modelling and other solution options are also mentioned. We have not yet found detailed information in the literature about the milling of HPL material, and our results are therefore new and necessary.

Keywords: milling; HPL—high-pressure laminate; measuring the load on the machine tool; CNC; milling; quality of the machined surface; statistics; histograms of loads

1. Introduction

Machining is one of the most important and widely used manufacturing technologies [1]. Traditional machining methods include milling, which is the chip machining of material with a multitool, where the cutting speed is determined by the rotation of the cutter around a fixed axis, and the feed rate is given by the movement of the workpiece.

The cutting speed and feed rate are vector quantities; depending on the direction of the vectors, we can distinguish between down milling (in which the vectors have the same direction) and up milling (in which the vectors have opposite directions). It is well known

that both of these techniques entail different machining flow during the cutting process. In particular, there are changes in cutting forces and temperature gradients during milling [2,3], which will affect the overall integrity and quality of the machined surface [4–6].

The subjects of this article are measurements performed on a selected machine tool, which is a new milling cutter with brazed cutting edges, under defined cutting conditions in down milling and up milling. The material to be machined is high-pressure plastic–laminate composite material, HPL, which is often used in both the construction and furniture industries. High-pressure laminates generally consist of fibrous reinforcing materials and resin binders, where the combination of heat and pressure produces a highly durable product. They can also be produced with antimicrobial properties [5,7–9].

The solution was realised at the Department of Applied Mechanics and at the Department of Machining, Assembly and Engineering Metrology, Faculty of Mechanical Engineering, VSB—Technical University of Ostrava (Ostrava, Czech Republic) in cooperation with the company VYDONA s.r.o. (Holešov, Czech Republic), which produces machine tools [7,10–12].

The obtained results, i.e., the force and moment load of the tool used and the quality of the machined surface, expressed by the achieved surface roughness, are statistically evaluated and displayed using bounded frequency histograms with their stochastic parameters. The results can be used practically, in design, strength analysis, and in the determination of the service life of cutting machines and machining tools, or the setting of optimal production technology. There is not enough information about the statistical evaluation of HPL material machining. However, stochastic approaches applied in the branch of mechanical engineering are widely accepted and used.

Time records of force and moment loads on the tool during milling are a typical stochastic process in mechanics [13–18].

The motivation for this article was a general lack of information on the machining of HPL material. This article aims to fill this information gap. We did not find enough information in the literature and did not find any literature about the milling mechanics of HPL material.

Marginally, the article is also focused on the finite element solution as well as the material properties and design of cutting tools [19].

The contribution of this paper is mainly the evaluation of the surface quality of machined surfaces in addition to the measurement of dynamic loads in the cutting tool and its evaluation.

2. Materials and Methods

2.1. Machining Tool and Its Material

For milling, the machining tool (milling cutter) shown in Figure 1 and Table 1 was used. The shank milling cutter, which is manufactured under the trade name DPØ10 × 12/60, Z2, RH, S10, HW, is made of two materials. The body of the tool is made of sintered carbide. Two cutting edges made of polycrystalline diamond DP101206020 are soldered to the body of the tool [7,9]. The angles of the face on the side and back planes are 0°.

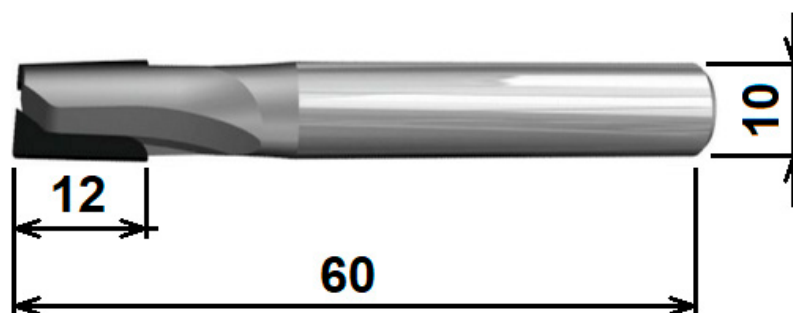


Figure 1. Shank milling cutter used for experiments.

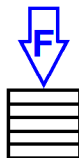

Table 1. Basic information about the machine tool and its material.

Cutter	Description and Dimensions of the Cutter	Shank Cutter Material	Material Properties of the Cutter			
			Young's Modulus/GPa/	Poisson's Ratio/1/	Yield Strength/MPa/	Ultimate Strength/GPa/
DPØ10 × 12/60, Z2,RH,S10,HW	Shank cutter with two soldered cutting edges	Tool (S10)	210	0.3	470 or more	-
		Cutting edge (polycrystalline diamond DP)	776	0.2	-	4.2–8

2.2. Machined Material

For numerical modelling using the finite element method (FEM) and for machining measurements, a high-pressure composite laminate (HPL) plate was used. The material properties of the orthotropic machined material are shown in Table 2. For more details, references [7,12] are given.

Table 2. Material properties of the machining material.

	Direction of Loading in Measurement	Young's Modulus/MPa/— Mean Value	Ultimate Strength/MPa/— Mean Value
High-pressure composite laminate (HPL)		1364	112.6
		1331	118.9

To obtain the properties of the orthotropic material, specific measurements were performed when the material was subjected to stress/strain states by bending; see [12].

2.3. Milling Machine

In the experiment, the DMU 50 2nd generation from DMG MORI with a rotary swivel table (range of the B-axis $-5/+110^\circ$), equipped with a Heidenhain ITNC 530 control system, was used, see Figure 2. It is a 5-axis system with a high-speed spindle, with a maximum speed of 18×10^3 rpm, a maximum spindle power of 21 kW, a table load of up to 300 kg and a large diameter of table bearings for highest precision. For more information, see [20–22].

2.4. Measuring Apparatus for Force and Torque Loading of the Tool during Milling

The main methods applied in this article are based on measurements and their evaluation. During milling, chips are separated from the base material under the action of the cutting force $F/N/$, which acts in the cutting zone and takes on a dynamic phenomenon, constantly changing in the time sequence, i.e., it has a stochastic (probabilistic, random) character. The technical term 'stochastic' in this case means the combination of statistics and probability theory in the dynamic and time-dependent problem of surface machining mechanics [23,24].

At the beginning of the cutting process, the force grows to a certain maximum at which a chip is formed. The shear force in the region of lower cutting speeds rises with increasing speed due to hardening of the deformation. Once the chip is separated from the base material, the cutting force decreases and the same process is followed to separate the next chip. In milling operations, the cross section of the chip changes during chip removal, which leads to a change in the components of the cutting forces. The magnitude

of the values of the cutting force components depends on the number of cutting edges that are engaged in the cut, and other cutting conditions. The resulting cutting force is the vector sum of the individual components of the forces acting on the workpiece. Moment components are generated in a similar way by the real interaction of the cutter and the workpiece, see [25].



Figure 2. Universal milling machine DMG MORI DMU 50.

The time records of the forces in the direction of the axes of the Cartesian coordinate system (F_x , F_y , and F_z /N/) and the moments around these axes (M_x , M_y , and M_z /Nm/) were measured during the milling. The resulting forces and moments were obtained by vector summing the corresponding quantities. These are of stochastic/probabilistic character, i.e., they are variables with natural variability.

A KISTLER type 9129AA piezoelectric three-component dynamometer was used, see [26], to measure the forces and moments of force and moment effects during milling. A KISTLER type 9129AA is a ‘universal’ dynamometer with a high natural frequency, main dimensions of $150 \times 107 \times 32$ mm, an accuracy of $\leq \pm 2\%$ of the measured range, and a maximum measuring range of ± 10 kN. Setup of this dynamometer enables accurate enough measurement of highly dynamic forces and guarantees very small influences of thermal effects [26].

Real-time force data from the dynamometer were transferred to a 5070A charge amplifier suitable for measurement with piezoelectric dynamometers or force plates. The signal was then sent to the data acquisition system DAQ BOX 5697A1. DAQ BOX 5697A1 is used for interfacing and controlling charge amplifiers and signal conditioners in general, as well as for cutting force applications using one or more component sensors and dynamometers, see [27]. Furthermore, it is processed using DynoWare software, which is capable of retrieving the necessary data at any time, and using them for further analysis. A schematic representation of the measurement of the cutting force components and their distribution is shown in Figure 3.

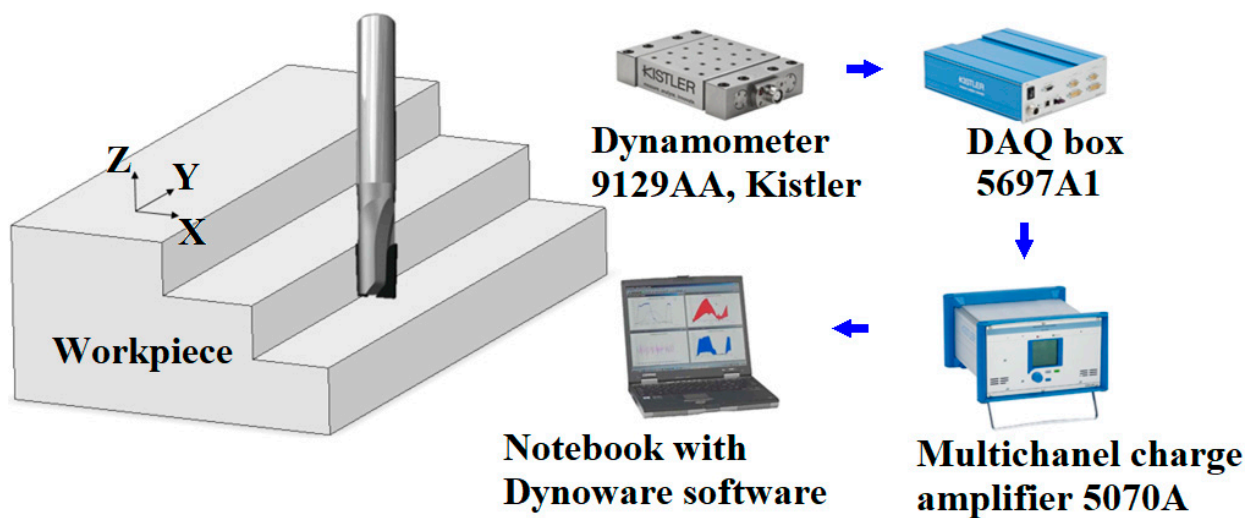


Figure 3. Cutting force distribution diagram and measuring equipment.

2.5. Defining Cutting Conditions during Milling

The correct selection of suitable cutting conditions always depends on the following input parameters:

- the type of material to be machined;
- cutting tool material and geometry;
- thermal conditions during machining;
- the required technological properties of the workpiece (dimensional accuracy, shape and quality of the machined surface).

More information about cutting conditions can be found in [28] and [29].

According to the milling cutter manufacturer and the selected new machine tool (trade name DPØ10 × 12/60,Z2,RH,S10,HW), the cutting conditions shown in Figure 4 were selected; for down milling, see Table 3, and for up milling, see Table 4.

A total of 36 measurements were taken and evaluated for constant speed and constant axial depth of cut. The other parameters varied, and are also shown in Tables 3 and 4. The entire milling experiment was carried out without the use of coolant.

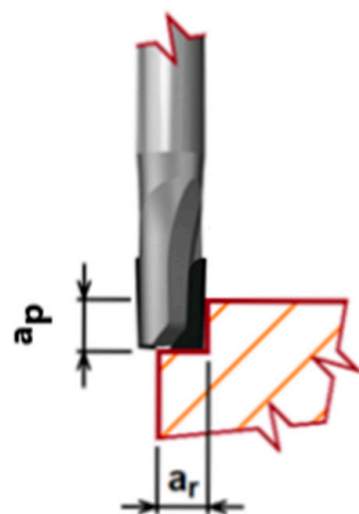


Figure 4. Definition of cutting parameters.

Table 3. Determination of cutting conditions for down milling.

Test No.	Feed per Tooth $f/mm/$	Radial Depth of Cut $a_r/mm/$	Axial Depth of Cut $a_p/mm/$	Spindle Speed $n/rpm/$	Type of Milling
1					
2	0.3				
3					
4		0.5			
5	0.6				
6					
7					
8	0.3				
9		0.75	5	18×10^3	Down milling
10					
11	0.6				
12					
13					
14	0.3				
15					
16		1			
17	0.6				
18					

Table 4. Determination of cutting conditions for up milling.

Test No.	Feed per Tooth $f/mm/$	Radial Depth of Cut $a_r/mm/$	Axial Depth of Cut $a_p/mm/$	Spindle Speed $n/rpm/$	Type of Milling
19					
20	0.3				
21					
22		0.5			
23	0.6				
24					
25					
26	0.3				
27		0.75	5	18×10^3	Up milling
28					
29	0.6				
30					
31					
32	0.3				
33					
34		1			
35	0.6				
36					

2.6. Measuring the Roughness of the Milled Surface

Measurement and evaluation of the roughness of the milled surface was carried out in accordance with the Czech standard ČSN EN ISO 4287, see [30]. For evaluation of the experimental activity, the two most commonly used parameters were selected; namely, the arithmetic mean deviation $R_a/\mu m/$ and maximum height $R_z/\mu m/$, or the sum of the

height of the highest profile protrusion and the depth of the lowest profile depression in the range of the basic length $l_r/\text{mm}/$. The following relationships apply:

$$R_a = \frac{1}{l_r} \int_0^{l_r} |Z(x)| dx, \quad (1)$$

$$R_z = Z_{pmax} + Z_{vmax}, \quad (2)$$

where $Z_{pmax}/\mu\text{m}/$ is the height of the highest peak of the profile and $Z_{vmax}/\mu\text{m}/$ is the depth of the highest depression.

Surface roughness measurement is part of surface integrity research, and is an important parameter of interest to the customer.

Surface roughness was measured at 6 locations for the up milling (points 1–6) and 3 locations for the down milling (points 7–9). Measurements were taken at nine locations, see Figure 5, in both the transverse and longitudinal directions. At each of the points, the measurement was performed three times, and subsequently the average value was considered. Measurement of the roughness of the machined material was carried out on an Alicona Infinite Focus G5 optical microscope [31]. A $20\times$ magnifying lens was used for the measurements.

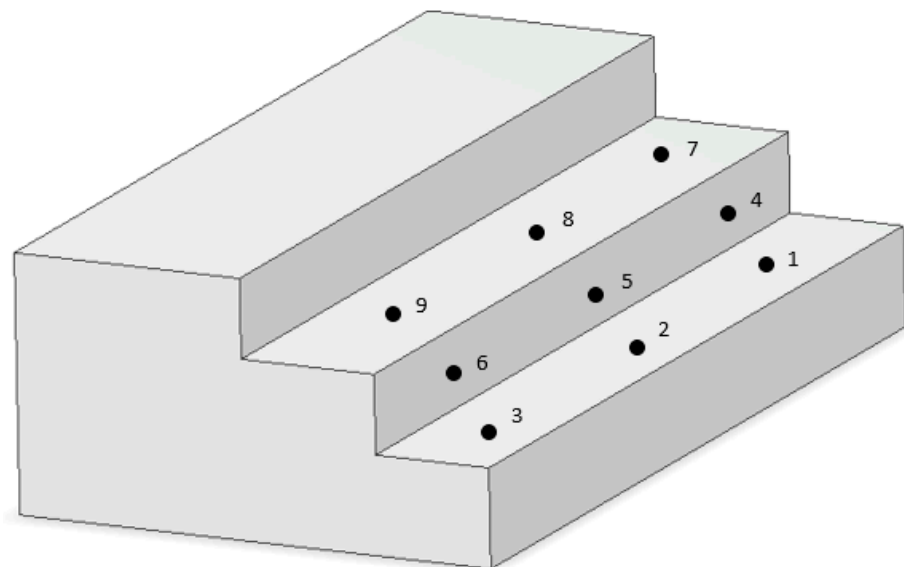


Figure 5. Measured points to evaluate the roughness of the milled surface. Points 1 to 6 were measured for up milling at $f = 0.6$ mm feed, and points 7 to 9 for down milling at $f = 0.6$ mm feed.

The integrity of the machined surface was satisfactory.

2.7. Statistical Data Processing of Milling

The measured stochastic data were evaluated in the usual way using Microsoft Excel software [32]. To make sure, the results were also checked by Anthill software [33]. The respective minimum (global minimum points), maximum (global maximum points), modes (value that appears most often in a set of data), medians (value separating the higher half from the lower half of a data), standard deviations and frequencies were determined to create bounded (truncated) bar histograms for the respective cutting conditions defined in Section 2.4. For more information, see [14–17,34].

For the dynamic measurement of forces and moments generated during milling, only the ‘steady state’—albeit time dependent—was statistically processed, i.e., the start and end of milling were not examined (as there were lesser loadings).

2.8. Note

We also performed vibration diagnostics by measurement, and the obtained results are reported in [12]. Due to the scope and significance of the paper, we decided to publish only the measurements of forces and moments during machining. In the future, we will also publish the results of the vibration diagnostics.

3. High-Pressure Laminate HPL Milling Results

In accordance with the previous text in Chapter 2, measurements were made and the results are presented in the following text.

3.1. Evaluation of the Measurement of Forces and Moments during Milling

An example of the time recording of the result of the measurement of the forces F_x , F_y , and F_z , and the moments M_x , M_y , and M_z during machining (i.e., measurement 1; for successive machining, see Table 3) can be seen in Figure 6.

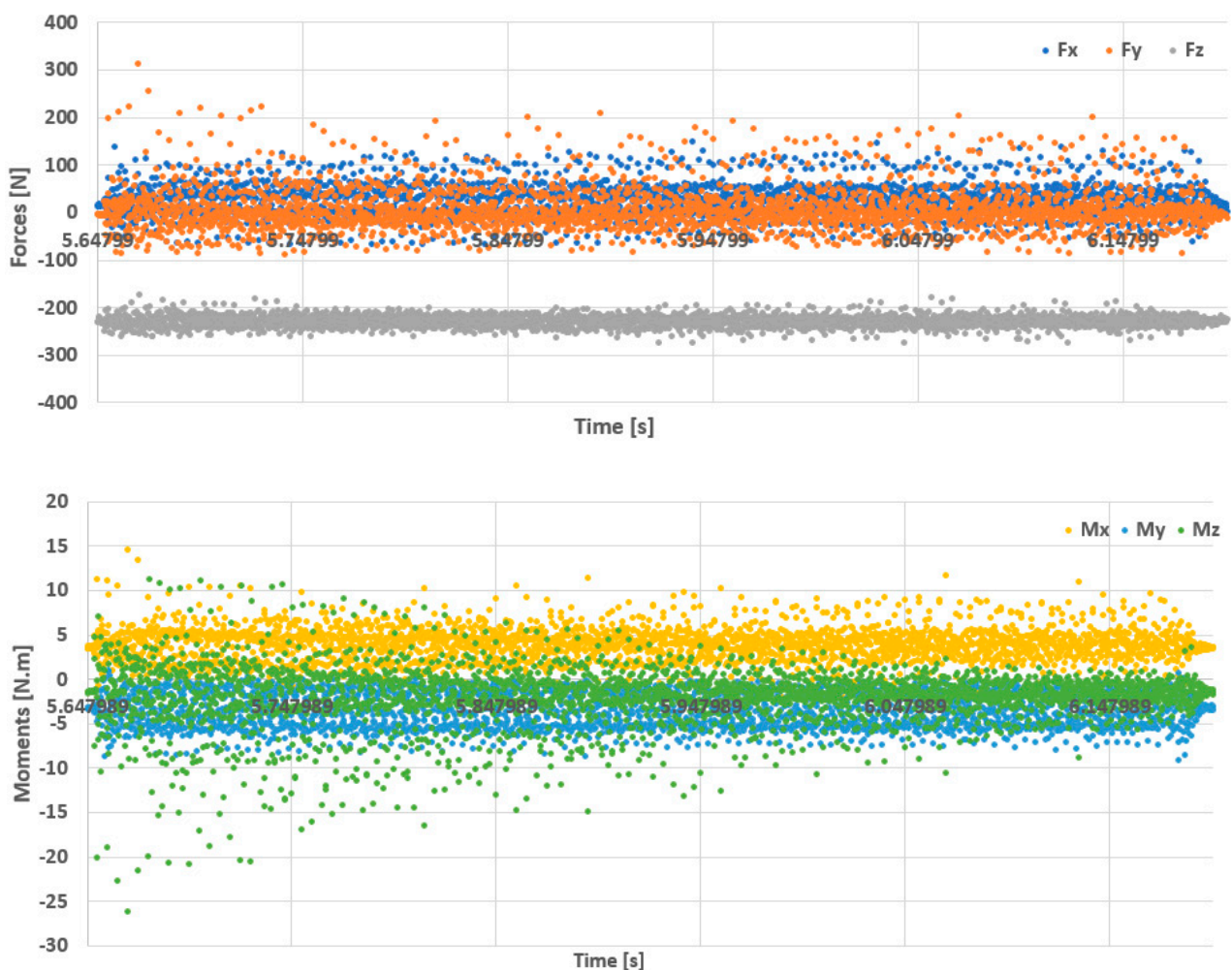


Figure 6. Time record of the result of the measurement of the forces F_x , F_y and F_z and the moments M_x , M_y and M_z during milling of the HPL (measurement 1; for down milling, see Table 3).

The time record of the values shown in Figure 6 can be statistically evaluated, see Table 5, where

$$F = \sqrt{F_x^2 + F_y^2 + F_z^2} \text{ and } M = \sqrt{M_x^2 + M_y^2 + M_z^2} \quad (3)$$

Table 5. Statistical evaluation of the partial forces F_x , F_y , F_z , the resulting forces F , the partial moments M_x , M_y , M_z , and the resulting moments M (measurement 1).

	Min	Mean	Modus	Median	Max	Standard Deviation
$F_x/N/$	-66.528	23.257	-0.610	16.022	148.926	34.555
$F_y/N/$	-86.365	6.868	-5.188	-1.526	314.331	45.418
$F_z/N/$	-274.353	-228.34	-223.389	-228.271	-172.119	12.126
$F/N/$	173.225	236.158	-	232.743	389.2558	18.976
$M_x/Nm/$	-2.2963	3.941	4.192	4.007	14.595	1.916
$M_y/Nm/$	-9.07379	-3.413	-5.056	-3.399	1.037	1.947
$M_z/Nm/$	-26.1569	-2.023	-1.393	-1.602	11.363	3.455
$M/Nm/$	0.481	6.552	-	6.058	30.065	2.784

From the statistical file, it is possible to create, for example, frequency histograms for the abovementioned quantities, e.g., for the forces F_x , F_y , F_z , see Figures 7–9 (measurement 1).

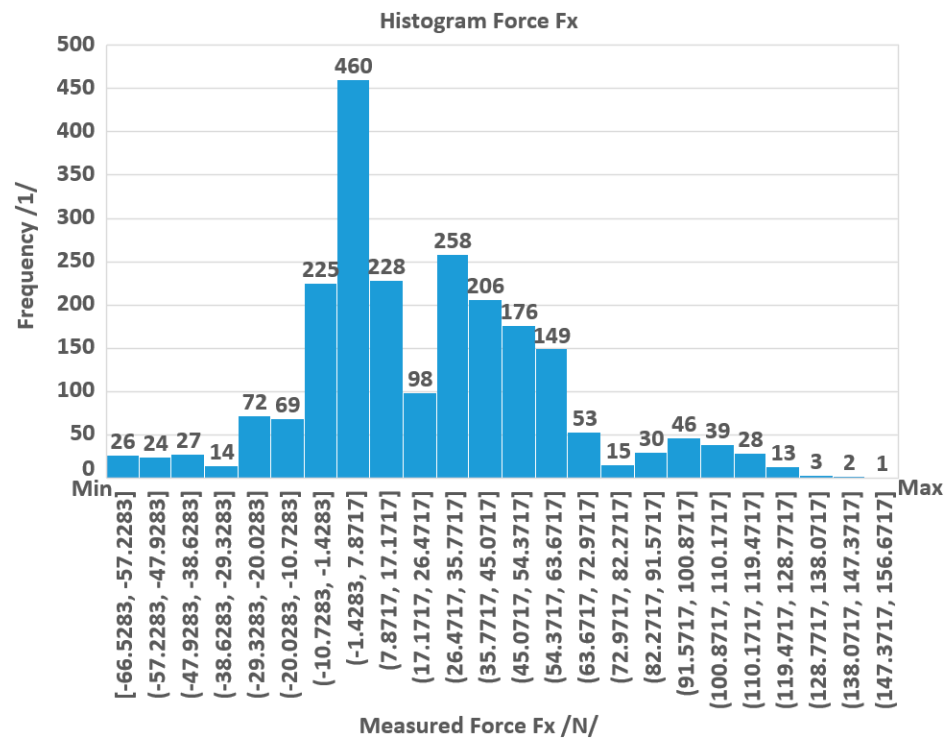


Figure 7. Histogram of the F_x force when milling HPL material (measurement 1; for down milling, see Table 3).

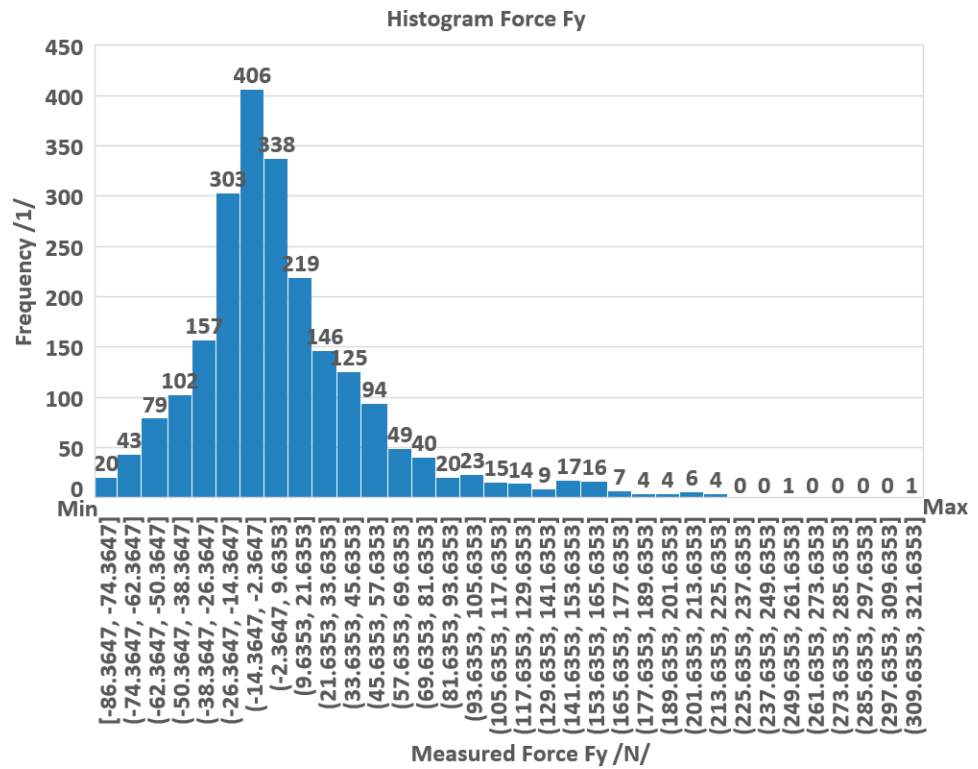


Figure 8. Histogram of the force Fy when milling HPL material (measurement 1; for down milling, see Table 3).

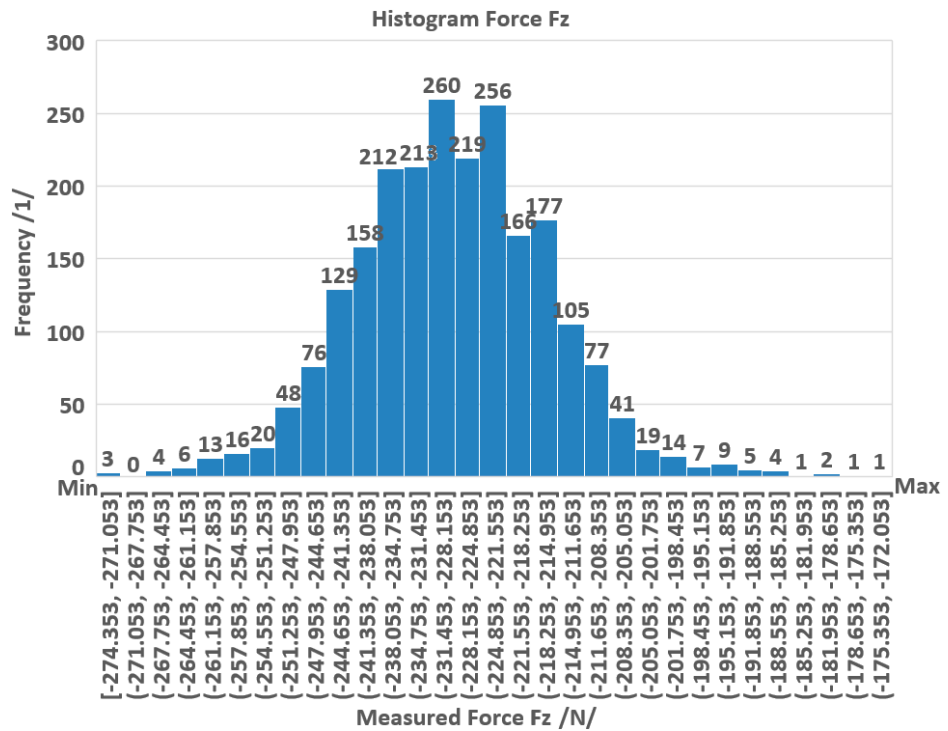


Figure 9. Histogram of the force Fz when milling HPL material (measurement 1; for down milling, see Table 3).

All 36 measurements can also be evaluated in a similar way. The basic statistical evaluation of the resultant forces and moments for all measurements is given in Tables 6 and 7,

where the evaluated median and maximum magnitudes of the resultant forces F and the resultant moments M during milling are given.

Table 6. Median and maximum values of the resulting forces and moments in down milling (measurements 1 to 16).

Measurement	F Median/N/	F Max/N/	M Median/N.m/	M Max/N.m/
1	243.589	319.714	6.049	18.328
2	242.498	312.381	6.010	16.779
3	243.993	363.700	6.053	18.804
4	246.792	360.623	6.361	17.762
5	246.680	344.163	6.3507	18.026
6	246.391	345.119	6.387	16.131
7	245.716	378.326	6.394	23.679
8	246.021	318.244	6.411	19.536
9	245.333	305.692	6.243	16.541
10	247.584	370.915	6.646	18.060
11	248.067	383.368	6.706	20.172
12	247.806	367.008	6.665	20.883
13	247.718	324.042	6.554	16.576
14	248.357	322.208	6.480	16.720
15	248.728	331.442	6.479	14.393
16	252.655	433.621	7.128	33.623
17	251.738	473.116	7.093	32.363
18	251.179	504.853	7.111	28.805

Table 7. Median and maximum values of resulting forces and moments in up milling (measurements 17 to 36).

Measurement	F Median/N/	F Max/N/	M Median/N.m/	M Max/N.m/
19	232.743	389.256	6.0585	30.065
20	238.341	398.425	6.426	30.679
21	240.161	396.847	6.155	30.905
22	248.143	488.090	7.536	32.542
23	247.513	527.396	7.401	43.184
24	244.958	587.898	7.788	46.012
25	242.623	424.391	6.460	35.308
26	242.914	429.885	6.432	33.719
27	242.298	392.560	6.341	29.817
28	249.071	652.812	8.187	55.177
29	253.026	686.911	7.792	58.015
30	253.872	487.237	7.977	36.992
31	244.786	448.866	6.553	36.568
32	245.622	399.778	6.715	30.903
33	246.173	371.328	6.853	27.431
34	253.839	725.676	8.282	55.628
35	256.515	585.917	8.860	43.214
36	254.625	577.478	8.765	45.329

Even if the number of measurements is small, the data from Tables 6 and 7 can be interleaved (approximated) with a quadratic surface for initial observation of trends. The most appropriate approximation appears to be the function:

$$f(f, a_r) = p_{00} + p_{10}f + p_{01}a_r + p_{11}f a_r + p_{02}a_r^2 \tag{4}$$

where p_{ij} (for $i = 0, 1$ and $j = 0, 1, 2$), are fitting constants.

An example of the interleaving of these quadratic surfaces for median values of force F can be seen in Figure 10 (down milling) and in Figure 11 (up milling), which were obtained using sw Matlab 2022a in ‘Surface fitting’ toolbox [35].

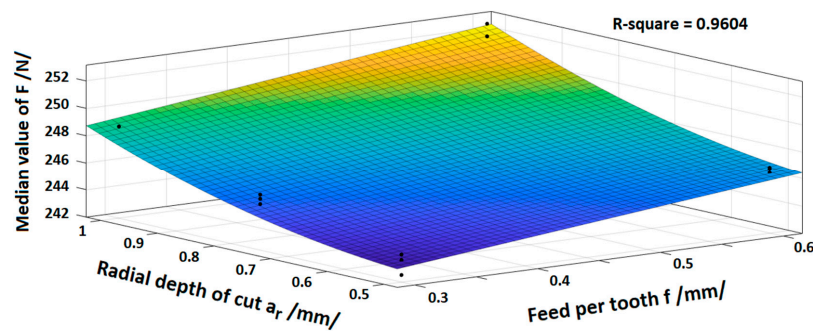


Figure 10. Fitting for median values of the resulting force F in down milling (measurements 1 to 16, Table 6).

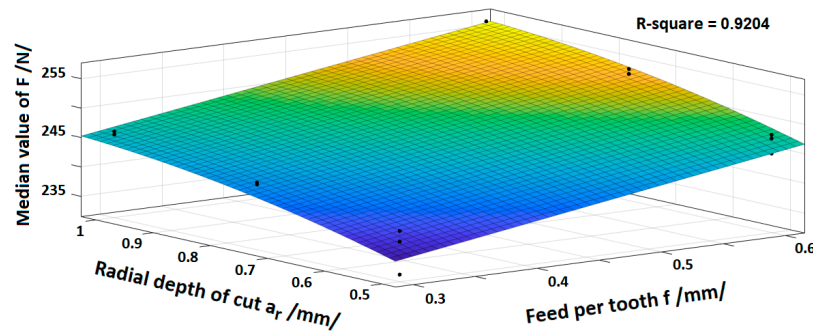


Figure 11. Fitting for median values of the resulting force F in up milling (measurements 17 to 32, see Table 7).

From these measurement results, the global maxima of the resulting forces and moments for successive and up milling are evident. These maxima are shown in Table 8 and were obtained by evaluating the local maxima shown in Tables 5 and 6.

Table 8. Global maximum values of the resultant forces and moments for down milling and up milling (evaluation of measurements 1 to 36).

Milling	F Max (Global Value)		M Max (Global Value)	
	Value/N/	Measurement	Value/Nm/	Measurement
Down milling	473.116	17	33.623	16
Up milling	725.676	34	55.628	34

The values in Table 8 provide new and valuable information on the actual dynamic loading of the cutting tool or workpiece during milling. It is clear from the above that up milling with the same cutting conditions results in higher force and moment loads than down milling with the same parameters.

3.2. Evaluation of Milling Surface Roughness Measurement

The roughness parameters R_a and R_z of the milled workpiece were evaluated in the longitudinal and transverse directions at predefined measuring points, see Equations (1), (2) and Figure 5. The values obtained for the parameter R_a are recorded in Table 9 and for the parameter R_z in Table 10.

Table 9. Results of R_a roughness measurement of milled surface of milled HPL material.

Point of Measurement, See Figure 5	Measurement Direction	$R_a/\mu\text{m/}$				
		Value	Mean	Standard Deviation		
1	Transverse	0.333	1.012	0.465	0.603	0.294
	Longitudinal	0.425	0.294	0.410	0.376	0.059
2	Transverse	0.501	0.452	0.335	0.429	0.070
	Longitudinal	0.509	0.452	1.064	0.675	0.276
3	Transverse	0.467	0.452	0.732	0.550	0.129
	Longitudinal	1.450	0.536	0.368	0.785	0.475
4	Transverse	1.338	1.385	1.376	1.366	0.020
	Longitudinal	0.607	0.594	0.734	0.645	0.063
5	Transverse	1.263	1.238	1.366	1.289	0.055
	Longitudinal	0.793	0.604	0.793	0.730	0.089
6	Transverse	1.257	1.113	1.203	1.191	0.059
	Longitudinal	0.617	1.296	0.825	0.913	0.284
7	Transverse	0.328	0.340	0.606	0.425	0.128
	Longitudinal	0.325	0.417	0.534	0.425	0.086
8	Transverse	0.725	0.222	0.631	0.526	0.218
	Longitudinal	0.289	0.837	0.371	0.499	0.241
9	Transverse	0.526	0.331	0.318	0.392	0.095
	Longitudinal	0.476	0.525	1.923	0.975	0.671

Table 10. Results of R_z roughness measurement of milled surface of milled HPL material.

Point of Measurement, See Figure 5	Measurement Direction	$R_z/\mu\text{m/}$				
		Value	Mean	Standard Deviation		
1	Transverse	1.897	4.748	3.637	3.427	1.173
	Longitudinal	2.077	1.525	1.815	1.806	0.276
2	Transverse	2.606	1.781	1.671	2.019	0.417
	Longitudinal	2.398	1.926	3.620	2.648	0.874
3	Transverse	1.727	2.052	2.563	2.114	0.344
	Longitudinal	4.704	2.228	2.009	2.980	1.497
4	Transverse	2.731	2.987	2.987	2.902	0.121
	Longitudinal	2.003	2.034	2.900	2.312	0.509
5	Transverse	4.116	3.133	4.081	3.777	0.455
	Longitudinal	3.716	2.539	2.724	2.993	0.633
6	Transverse	3.622	2.813	3.006	3.147	0.345
	Longitudinal	2.357	4.916	3.764	3.679	1.282
7	Transverse	1.624	1.667	2.315	1.869	0.316
	Longitudinal	1.563	2.001	1.991	1.852	0.250
8	Transverse	3.344	0.991	2.231	2.189	0.961
	Longitudinal	1.367	2.556	2.046	1.990	0.596
9	Transverse	1.75	1.237	1.185	1.391	0.255
	Longitudinal	2.668	2.073	6.920	3.887	2.643

In general, the surface roughness is higher in the up milling than in down milling. This is also true for HPL material, as can be seen from the results in the graphs in Figures 12 and 13. Up milling achieves a significantly higher profile parameter R_z , compared with down milling in both transverse and longitudinal directions.

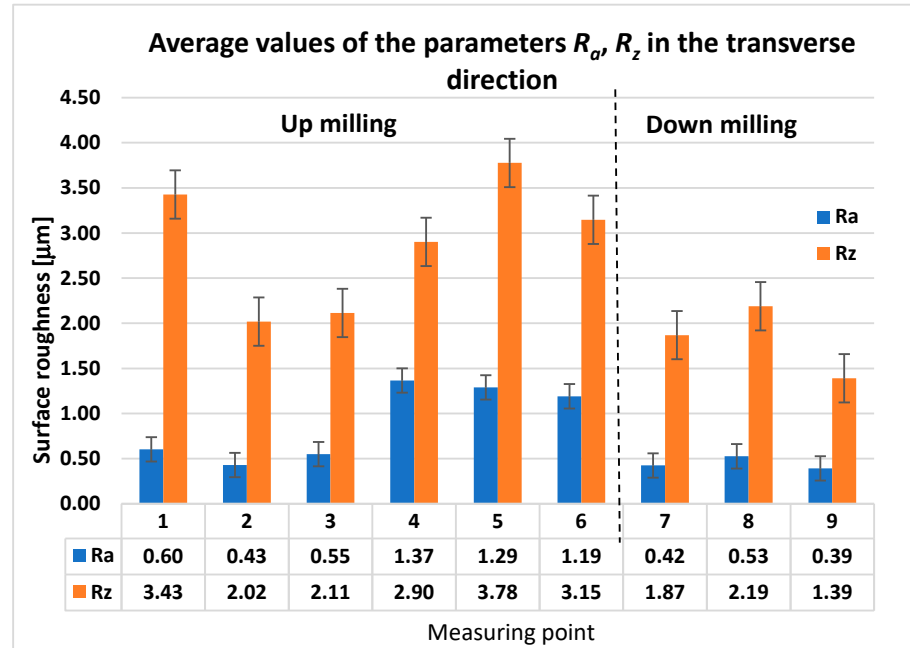


Figure 12. Average values of the parameters R_a , and R_z in the transverse direction.

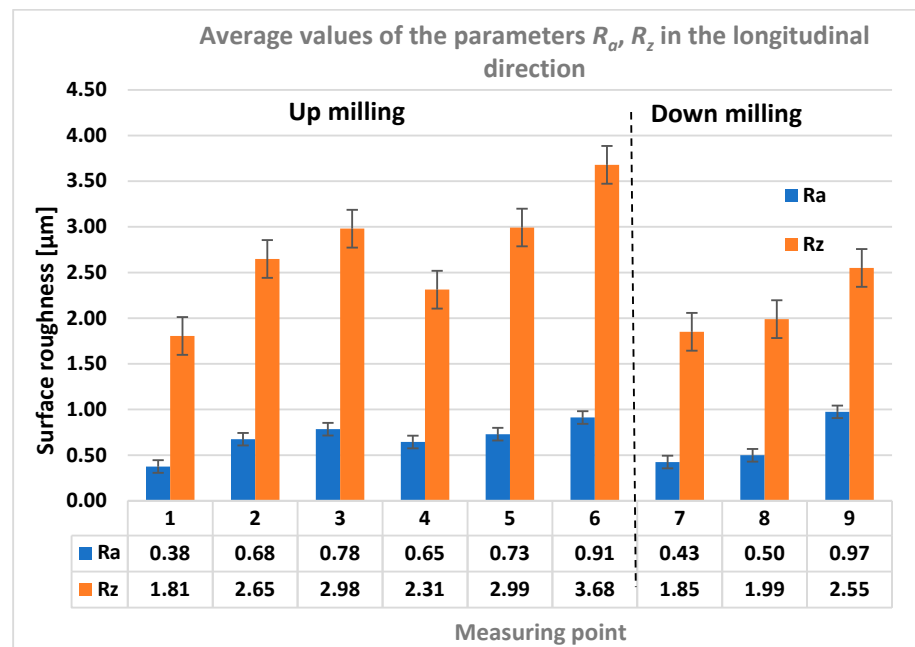


Figure 13. Average values of the parameters R_a , and R_z in the longitudinal direction.

The measured values of the roughness parameter R_a of the HPL surface ranged from 0.222 to 1.385 μm in the transverse direction, and from 0.289 to 1.923 μm in the longitudinal direction for down milling. For up milling, the range of parameter R_a was 0.991 to 4.748 μm in the transverse direction, and 1.367 to 6.92 μm in the longitudinal direction.

The obtained results have not yet been published in the literature outside of our work, and can be used not only for numerical modelling but also for engineering design or optimisation of new machine tools; see e.g., Section 4.

4. Concise Information on the Strength Analysis of Milling Cutters

Strength analysis is not the main topic of this article, but it is related to the direct application of the obtained measurements. Therefore, it is appropriate to briefly mention it here.

The results of the force and moment measurements from Section 3.1 can be used as boundary conditions for numerical simulation using the Finite Element Method (FEM), see e.g., references [36,37]. An example of the solution result, the calculation of the mechanical stress in a shank mill during milling, is shown in Figure 14. The results of the FEM solution can be used in design and mill optimisation and will be fully published in the future.

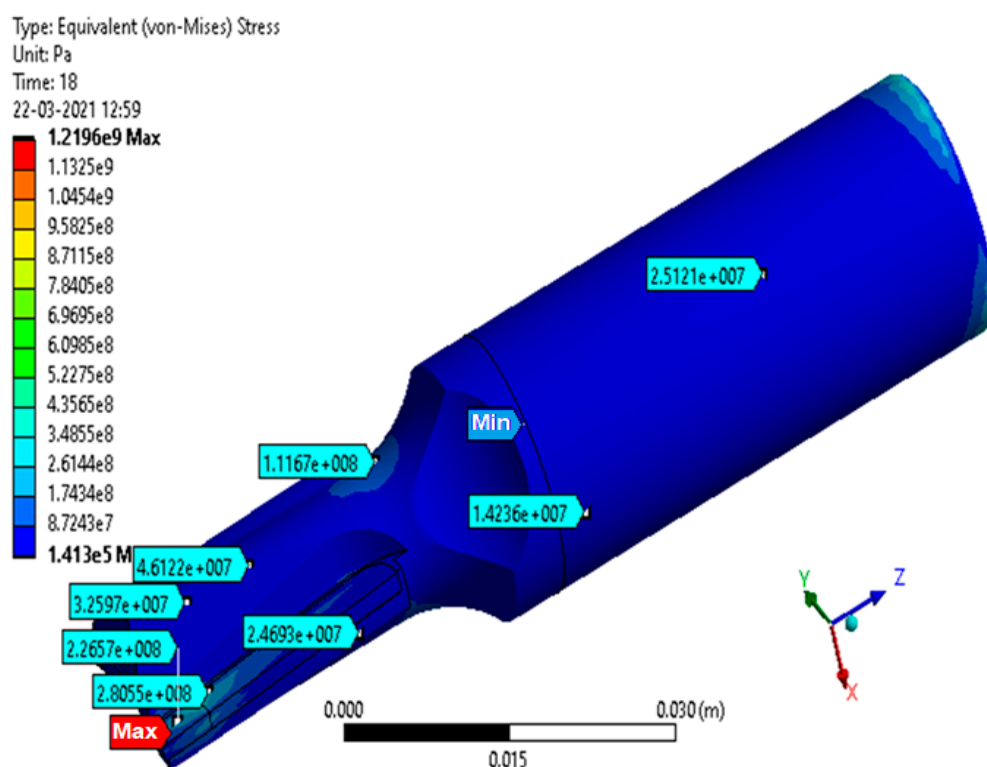


Figure 14. Example of the calculation of equivalent von Mises stress using the Finite Element Method (ANSYS software).

Knowledge of the force and moment loads of both tool and workpiece as well as the quality of the machined surface is important for the design and development of machine tools.

5. Discussion

Currently, not enough information is known about the milling of nontraditional materials, such as the HPL high-pressure composite laminate that we have designed. For this reason, this paper is a positive contribution and presents new information.

From the evaluation of the loads during down and up milling, i.e., the time records of forces and moments (for example, maximum values 473.1 N and 33.623 Nm for down milling, and 725.7 N and 55.628 Nm for up milling etc., see Tables 5–8), it was possible to evaluate the real dynamic loads using statistics, including the creation of bounded histograms for further use. The statistical records can also be used in real stochastic

modelling of the milling process or other experiments, or for numerical modelling using FEM in connection with designing, see Figure 14. For more details, see [38–41].

The same is true for the statistical evaluation of the roughness of the milled surface (for example, the maximal values of surface roughness Ra and Rz are 1.385 and 6.920, respectively; for up milling, see Tables 9 and 10).

The Monte Carlo Method or other stochastic approaches can be applied. For more details, see [38,39,42] and [43].

The next step can also be to investigate other dynamic characteristics such as vibrations during milling and modal analysis of the machine, tool, materials and workpiece system [40–48]. A basic vibration diagnostic measurement was also performed, but the results will be published in the future.

The practical design of machine tools and the setting of appropriate cutting conditions are also aimed at improving the quality and integrity of the machined surface. Applications of stochastic (probabilistic) methods are also appropriate in this area. See [41,42,49,50].

The main innovation of the publication is the determination of the force and moment load on the tool (cutter) or workpiece during milling, in relation to the cutting conditions and surface roughness of the HPL material being machined; see Section 3. It is clear that the dynamic loading of the tool or workpiece with the same cutting conditions results in higher force and moment loads for up milling than down milling with the same parameters. Surface quality, or lower surface roughness, is better with down milling.

These results indicate a preference for down milling during machining of HPL material.

The results obtained have been and can be used in the design of machine tools or their optimisation, see Figures 1, 4 and 14.

This methodology can also be applied to other machining methods and other machined materials.

6. Conclusions

It was possible to implement and evaluate 36 real milling cases under different cutting conditions. Time–force and time–moment records of the dynamic loading during milling were obtained. The roughness of the machined surface was also investigated. The results obtained were statistically evaluated and can be used not only in further research, but also for setting the optimal cutting conditions of milling technology, strength analyses, and design and optimisation of milling machines.

The method of measurement and processing of the results is explained.

An example of an application on a new cutter design (DPØ10 × 12/60, Z2, RH, S10, HW) is used in the application of the finite element method and engineering design.

A similar procedure can be used to solve machining tasks, with other tools, for other types of machine tools and other types of materials.

It is clear that the dynamic loading forces and moments are greater in up milling than down milling. Furthermore, the surface quality and integrity is better in down milling. From these results, it is recommended to choose down milling during the machining of HPL material.

There is a lack of technical information regarding the milling of plastics and especially the machining of the material HPL. We have not yet found any scientific publications on this topic. For this reason, the article fills at least part of the information gap.

Author Contributions: Conceptualization, K.F. and I.M.; Methodology, I.M., K.F. and J.K.; Validation, P.K.; Formal analysis, A.S., R.M. and D.S.; Investigation, K.F., O.S., I.M., T.J., M.V., R.M., J.P. and J.H.; Data curation, K.F., O.S., A.S., J.K., M.V. and J.H.; Writing—original draft, K.F., O.S., A.S. and T.J.; Writing—review & editing, K.F.; Supervision, J.K. and M.H.; Project administration, K.F., I.M., M.V. and M.H. All authors have read and agreed to the published version of the manuscript.

Funding: This article was supported by Czech projects SP2022/26, SP2022/50 This article was supported by Czech projects CZ.01.1.02/0.0/0.0/19_262/0020149, CZ.02.1.01/0.0/0.0/17_049/0008441 and CZ.02.1.01/0.0/17_049/0008407 within the Operational Programme Research, Development and Education financed by the European Union and from the state budget of the Czech Republic.

Institutional Review Board Statement: Not applicable.

Informed Consent Statement: Not applicable.

Data Availability Statement: Not applicable.

Conflicts of Interest: The authors declare no conflict of interest.

References

1. Sreejith, P.S.; Ngoi, B.K.A. Dry machining: Machining of the future. *J. Mater. Process. Technol.* **2000**, *101*, 287–291. [CrossRef]
2. San-Juana, M.; Martina, Ó.; Tiedra, M.P.; Santos, F.J.; López, R.; Cebrián, J.A. Study of cutting forces and temperatures in milling of AISI 316L. *Proc. Eng.* **2015**, *132*, 500–506. [CrossRef]
3. Nemetza, A.W.; Davesae, W.; Klünsner, T.; Praetzasb, C.; Liuc, W.; Tepperneggd, T.; Czettld, C.; Haasc, F.; Böllingb, C.; Schäfer, J. Experimentally validated calculation of the cutting edge temperature during dry milling of Ti6Al4V. *J. Mater. Process. Technol.* **2020**, *278*, 116544. [CrossRef]
4. Li, B.; Yan, Y.; Yang, J. Influence and optimization criterion of milling modes and process parameters on residual stress. In Proceedings of the 5th International Conference on Advanced Design and Manufacturing Engineering, Shenzhen, China, 19–20 September 2015; Atlantis Press: Amsterdam, The Netherlands; pp. 1874–1879. [CrossRef]
5. Laamouri, A.; Ghanem, F.; Braham, C.; Sidhom, H. Influences of Up-Milling and Down-Milling on Surface Integrity and Fatigue Strength of X160CrMoV12 Steel. *Int. J. Adv. Manuf. Technol.* **2019**, *105*, 1209–1228. [CrossRef]
6. Smith, D.J.; Farrahi, G.H.; Zhu, W.X.; McMahon, C.A. Experimental measurement and finite element simulation of the interaction between residual stresses and mechanical loading. *Int. J. Fatigue* **2001**, *23*, 293–302. [CrossRef]
7. Vydoná. Available online: <https://www.vydoná.cz/english.html> (accessed on 5 December 2022).
8. Magina, S.; Santos, M.D.; Ferra, J.; Cruz, P.; Portugal, I.; Evtuguin, D. High Pressure Laminates with Antimicrobial Properties. *Materials* **2016**, *9*, 100. [CrossRef]
9. Technical Characteristics and Physical Properties of HPL. Available online: https://www.pro-hpl.org/assets/uploads/prohpl/files/TL_150623_technical_characteristics_and_physical_properties_of_HPL.pdf (accessed on 5 December 2022).
10. Department of Applied Mechanics. Available online: <https://www.fs.vsb.cz/330/en> (accessed on 5 December 2022).
11. Department of Machining, Assembly and Engineering Metrology. Available online: <https://www.fs.vsb.cz/346/en> (accessed on 5 December 2022).
12. Frydryšek, K.; Mrkvica, I.; Skoupý, O. *Znalecký posudek ZD-59/300/FS-DV (Vývoj 3 nových generací vícebřitých sekčních nástrojů s ohledem na výzkum procesních vlivů při obrábění) Expert's opinion written in Czech language; (In Czech language); Faculty of Mechanical Engineering, VSB—Technical University of Ostrava: Ostrava, Czech Republic, 2021; pp. 1–107.*
13. Schulze, V. *Modern Mechanical Surface Treatment: States, Stability, Effects*; John Wiley & Sons: Hoboken, NJ, USA, 2006.
14. Vlčková, K.; Frydryšek, K.; Bajtek, V.; Demel, J.; Pleva, L.; Havlíček, M.; Pometlová, J.; Madeja, R.; Kratochvíl, J.; Krpec, P.; et al. Analytical, Stochastic and Experimental Solution of the Osteosynthesis of the Fifth Metatarsal by Headless Screw. *Appl. Sci.* **2022**, *12*, 9615. [CrossRef]
15. Frydryšek, K.; Šír, M.; Pleva, L.; Szeliga, J.; Stránský, J.; Čepica, D.; Kratochvíl, J.; Koutecký, J.; Madeja, R.; Dědková, K.P.; et al. Stochastic Strength Analyses of Screws for Femoral Neck Fractures. *Appl. Sci.* **2022**, *12*, 1015. [CrossRef]
16. *Probabilistic Assessment of Structures Using Monte Carlo Simulation, Background, Exercises and Software*, 2nd ed.; Marek, P.; Brozzetti, J.; Guštar, M.; Tikalsky, P. (Eds.) Institute of Theoretical and Applied Mechanics, Academy of Sciences of Czech Republic: Prague, Czech Republic, 2003; ISBN 80-86246-19-1.
17. Tvrdá, K. Probability and Sensitivity Analysis of Plate. *Appl. Mech. Mater.* **2014**, *617*, 193–196. [CrossRef]
18. High Pressure Laminate (HPL)—Material Intelligence. Available online: <https://www.materialintelligence.com/hpl> (accessed on 5 December 2022).
19. Jeulin, M.; Cahuc, O.; Darnis, P.; Laheurte, R. A 6-components mechanistic model of cutting forces and moments in milling. *Forces Mech.* **2022**, *9*, 100130. [CrossRef]
20. Kumar, D.; Gururaja, S. Machining damage and surface integrity evaluation during milling of UD-CFRP laminates: Dry vs. cryogenic. *Compos. Struct.* **2020**, *247*, 112504. [CrossRef]
21. Sílvia, R.-C.; Lauro, C.H.; Horovistiz, A.; Davim, J.P. Development of FEM-based digital twins for machining difficult-to-cut materials: A roadmap for sustainability. *J. Manuf. Process.* **2022**, *75*, 739–766. [CrossRef]
22. DMG MORI DMU 50. Available online: <https://uk.dmgmori.com/products/machines/milling/5-axis-milling/dmu/dmu-50-2nd-generation> (accessed on 5 December 2022).
23. Is There a Difference between Stochastic and Probabilistic? Available online: <https://www.quora.com/Is-there-a-difference-between-Stochastic-and-Probabilistic> (accessed on 5 December 2022).

24. Category:Stochastic Processes—Wikipedia. Available online: https://en.wikipedia.org/wiki/Category:Stochastic_processes (accessed on 5 December 2022).
25. Insperger, T.; Mann, B.P.; Stépán, G.; Bayly, P.V. Stability of Up-Milling and Down-Milling, Part 1: Alternative Analytical Methods. *Int. J. Mach. Tools Manuf.* **2003**, *43*, 25–34. [CrossRef]
26. Compact Multi-Component Dynamometer Kistler 9129AA. Available online: <https://www.kistler.com/en/product/type-9129aa/> (accessed on 5 December 2022).
27. Data Sheet, Type 5697A kistler.com. Available online: <https://www.kistler.com/files/document/000-745e.pdf> (accessed on 1 November 2022).
28. Pontius, K.R. New Veins of Application. *Cut. Tool Eng.* **2002**, *54*. Available online: https://www.ctemag.com/sites/www.ctemag.com/files/archive_pdf/0208-veinsofapplication.pdf (accessed on 5 December 2022).
29. Degner, W.; Litze, H.; Smejkal, E.; Heisel, U.; Rothmund, J. *Spanende Formung; Theorie-Berechnung-Richtwerte*; Carl Hanser Verlag: München, Germany, 2019; ISBN 678-3-44645032-6.
30. ČSN EN ISO 4287 (014450). Available online: <https://www.technicke-normy-csn.cz/csn-en-iso-4287-014450-160147.html> (accessed on 1 November 2022).
31. Alicona InfiniteFocus G5. Available online: https://www.uphf.fr/LAMIH/sites/fr.LAMIH/files/images/Platforms/Morphomeca/EN/FICHES/Alicona_IF_G5.pdf (accessed on 1 November 2022).
32. Descriptive Statistics in Excel—Easy Tutorial—excel-easy.com. Available online: <https://www.excel-easy.com/examples/descriptive-statistics.html> (accessed on 5 December 2022).
33. SBRA-Software—noise.cz. Available online: <http://www.noise.cz/sbra/software.html> (accessed on 5 December 2022).
34. Famfulík, J.; Míková, J.; Lánská, M.; Richtář, M. A Stochastic Model of the Logistics Actions Required to Ensure the Availability of Spare Parts During Maintenance of Railway Vehicles. *Proc. Inst. Mech. Eng. Part F J. Rail Rapid Transit* **2014**, *228*, 85–92. [CrossRef]
35. Surface Fitting—MATLAB & Simulink—mathworks.com. Available online: <https://www.mathworks.com/help/curvefit/surface-fitting.html> (accessed on 5 December 2022).
36. Tekkaya, A.E.; Soyarslan, C. Finite Element Method. In *The International Academy for Production Engineering*; Laperrière, L., Reinhart, G., Eds.; CIRP Encyclopedia of Production Engineering; Springer: Berlin/Heidelberg, Germany, 2019. [CrossRef]
37. Astakhov, V.; Outeiro, J. Metal Cutting Mechanics, Finite Element Modelling. In *Machining*; Springer: London, UK, 2008; ISBN 978-1-84800-213-5. [CrossRef]
38. Lokaj, A.; Klajmonová, K. Comparison of behaviour of laterally loaded round and squared timber bolted joints. *Frattura ed Integrità Strutturale* **2016**, *11*, 56–61. [CrossRef]
39. Frydrýšek, K. Probabilistic Approaches Applied in the Solution of Problems in Mining and Biomechanics. In Proceedings of the 17th International Conference Engineering Mechanics 2011, Svratka, Czech Republic, 9–12 May 2011; pp. 151–154, ISBN 978-80-87012-33-8.
40. Cienciala, J.; Frydrýšek, K.; Podešva, J. Nonlinear Vibration—Stochastic Approach. In Proceedings of the 23rd International Conference Engineering Mechanics, Svratka, Czech Republic, 15–18 May 2017; Institute of Theoretical and Applied Mechanics of the Czech Academy of Sciences: Prague, Czech Republic, 2017. Available online: <https://www.webofscience.com/wos/woscc/full-record/WOS:000411657600054> (accessed on 5 December 2022).
41. Petru, J.; Zlámal, T.; Čep, R.; Monková, K.; Monka, P. Influence of Cutting Parameters on Heat-Affected Zone after Laser Cutting. *Tehnicki vjesnik/Technical Gazette* **2013**, *20*, 225–230.
42. Mrkvica, I.; Jurga, T.; Slaninkova, A.; Jurko, J.; Panda, A.; Krpec, P. Design of a ComputerAided Gear Manufacturing Tool—Rack-Shaped Cutter. *MM Sci. J.* **2021**, *5403*–5409. [CrossRef]
43. Bajaj, N.S.; Patange, A.D.; Jegadeeshwaran, R.; Kulkarni, K.A.; Ghatpande, R.S.; Kapadnis, A.M. A Bayesian Optimized Discriminant Analysis Model for Condition Monitoring of Face Milling Cutter Using Vibration Datasets. *ASME J. Nondestruct. Eval.* **2022**, *5*, 021002. [CrossRef]
44. Frydrýšek, K.; Čepica, D.; Halo, T. Biomechanics—Probabilistic Anthropometry Approach for Sitting Human and Seat. In *Experimental Stress Analysis—57th International Scientific Conference, EAN 2019—Conference Proceedings*; Czech Society for Mechanics: Praha, Czech Republic, 2019; pp. 90–96. ISBN 978-80-214-5766-9.
45. Vavrušová, K.; Mikolášek, D.; Lokaj, A.; Klajmonová, K.; Sucharda, O.; Parenica, P. Determination of Carrying Capacity of Steel-Timber Joints with Steel Rods Glued-In Parallel to Grain. *Wood Res.* **2016**, *61*, 733–740.
46. Malerová, L.; Pokorný, J.; Kristlová, E.; Wojnarova, J. Using of mobile flood protection on the territory of the Moldova as possible protection of the community. *IOP Conf. Ser. Earth Environ. Sci.* **2017**, *92*, 12039. [CrossRef]
47. Murčinková, Z.; Postawa, P.; Winczek, J. Parameters Influence on the Dynamic Properties of Polymer-Matrix Composites Reinforced by Fibres, Particles, and Hybrids. *Polymers* **2022**, *14*, 3060. [CrossRef] [PubMed]
48. Murčinková, Z.; Šmeringaiová, A.; Halapi, M. Damping properties of composites with short and long fibres by impact testing. *AIP Conf. Proc.* **2019**, *2077*, 020042. [CrossRef]
49. Hrabovský, L.; Mantič, M.; Voštová, V. Adhesion Coefficient on the Limit of Slippage at Star-Up of the Manual Crane Trolley. *Advances in Science and Technology. Res. J.* **2019**, *13*, 92–99. [CrossRef]
50. Hage, I.S.; Seif, C.Y.; Hamade, R.F. Cortical Osteon Stiffness: A Comparative Micromechanics-Based Homogenization Study. *Int. J. Multiscale Comput. Eng.* **2021**, *19*, 55–72. [CrossRef]